Supplement (E-PRLTAO-96-019605) to "Nuclear Emissions During Self Nucleated Acoustic Cavitation," by

R. P. Taleyarkhan[1*], C. D. West[2,3], R. T. Lahey, Jr.[4], R. I. Nigmatulin[5], R.C.Block [4,3], and Y. Xu[1]
[1]*Purdue University, West Lafayette, Indiana 47907, USA*
[2] *Oak Ridge National Laboratory, Oak Ridge, TN, 37830, USA*
[3]*Retired*
[4]*Rensselaer Polytechnic Institute, Troy, New York 12180, USA*
[5]*Russian Academy of Sciences, 6 Karl Marx Street, Ufa 450000, Russia*
(*)– Corresponding author (rusi@purdue.edu)

This supplement provides additional information and "raw" experimental data related to the manuscript *Nuclear Emissions During "Self" Nucleated Acoustic Cavitation*, by R. P. Taleyarkhan, C. D. West, R. T. Lahey,Jr., R. I. Nigmatulin, R. C. Block, and Y. Xu, *Physical Review Letters*, January, 2006.

Introduction

It is well known that the intense implosive collapse of bubbles, including acoustic cavitation bubbles, can lead to extremely high compressions and temperatures, and to the generation of light flashes attributed to sonoluminescence (SL). In addition, for suitable conditions and materials, we can also have nuclear emissions (*1a*). The modeling and analyses of the basic physical phenomena associated with such a process have been discussed in detail elsewhere *(1b,2,3)*. Essentially, the process starts with bubble implosion, during the compression phase of the impressed acoustic pressure field, when the gas/vapor interfacial Mach number $\left(\left|\dot{R}\right|/C_g\right)$ is much less than unity. As the interfacial Mach number approaches unity a compression shock wave is formed in the gas/vapor mixture and this shock wave moves toward the center of the bubble and, in doing so, intensifies. As the shock wave bounces off itself at the center of the bubble it highly compresses and heats a small core region near the center of the bubble. At this point we normally have a SL light pulse, and if we have a suitable (e.g., deuterated) liquid and the bubble temperatures, density and their duration are sufficient, we may also have conditions suitable for nuclear emissions (i.e., thermonuclear D-D fusion). The light and nuclear emissions and the pressurization process continues until a short time later when the interface comes to rest. Thereafter, we have the onset of bubble expansion during the rarefaction phase of the impressed acoustic pressure field, and a rarefying shock wave is formed in the liquid surrounding the bubble during the bubble growth process. As will be described later, for sufficiently violent implosions this shock wave is normally heard by the experimenters when it reaches the wall of the test section in which the experiment is being performed.

Our aim was to study the ultrahigh compression effects and temperatures in vapor bubbles nucleated in highly tensioned liquids by means of dissolved alpha emitters, whereby the bubble radius increases from an initial radius (R_o) of tens of nanometers to a maximum radius (R_m) in the millimeter range. The liquid's kinetic energy, which is accumulated during the implosion stage, and is subsequently converted to internal energy in and around the bubble, is given by $E = p_m R_m^3$. In typical sonofusion experiments (*1-*

4), p_m = 15 bar, R_m = 500 to 800 μm which leads 10^4 to 10^5 times more liquid phase kinetic energy, E, than in typical Single Bubble Sonoluminescence (SBSL) experiments (i.e., where: p_m = 1.5 bar, R_m = 50 μm). Such an approach, with its vastly increased energy concentration potential during implosions, gives rise to the potential for much higher peak temperatures and densities within the imploding bubbles, possibly leading to D-D fusion and detectable levels of nuclear particle emissions in suitable deuterated liquids. Indeed, we have previously presented evidence (*1a,2,3,4)* for 2.45 MeV neutron emission and tritium production during external neutron-seeded cavitation experiments with chilled deuterated acetone, and these observations have now been independently confirmed *(5).*

Notes on Test Cell Operational and Performance Aspects

In our earlier experiment using acetone, for bubble nucleation we utilized a fast neutron source (either a PNG which was synchronized to fire at the point of lowest pressure in the antinode), or a 1 Ci Pu-Be source. A unique feature of the present experiements was the method for bubble nucleation in which we utilized a dissolved alpha emitter uranyl nitrate *(13, 14)* in mixtures of water, benzene, tetrachloroethylene and acetone. In particular, randomly generated (mainly ~ 4 MeV alpha particles) from the radioactive decay of dissolved natural uranium was used to nucleate bubbles. This completely obviates the need to use an external neutron source and resolves any lingering confusion associated with the possible influence of the previously used *(1, 2)* external source neutrons on the emitted 2.45 MeV neutrons. Notably, this permitted us to develop and successfully test a unique, new stand-alone acoustic inertial confinement nuclear fusion test device. The experimental configuration utilized for the present study is shown in Figure 1.

Due to unavailability of a Pyrex™ test cell of the type used earlier *(1, 2)*, the tests reported in this manuscript were conducted in a somewhat larger test cell (outer diameter = 68 mm) made with quartz. While previously we could obtain roughly ~ 30 bubble cluster bursts per second with a pressure drive amplitude of ~ +/-15 bar (*1a,2*), for the present setup the nucleation rate that could be obtained with an external fast neutron source and the benzene mixture dropped to ~5 bubble bursts per second. Significantly, the use of dissolved uranyl nitrate, which emitted short range nucleating particles randomly in time, gave rise to bubble clusters at nucleation rates of only about 1 per second for a drive amplitude of up to +/- 15 bar. Moreover, the clusters were prone to gassy-like premature nucleation with an occasional tendency to generate non-spherical "comet-like" structures, at which point the nuclear emission signals dropped to background levels giving null results. The present self-induced nucleation experiments were necessarily conducted under these somewhat degraded conditions which yielded a reduced bubble nucleation rate and therefore, correspondingly resulted in reduced D-D neutron production rates. It is not clear at the present time why this sort of performance degradation takes place; **however, the aim of the present experiments was not to optimize D-D neutron emission but to assess if neutron-gamma emissions were at all possible during cavitation bubble implosions with deuterated liquids without the use of an external neutron source**. It is categorically cautioned also that the neutron output

can vary quite significantly and was found to be closely related to the departure from sphericity of the imploding bubbles.

Nuclear emissions with cavitation for a deuterated liquid can vary significantly and it is not uncommon to get null results on a given day if the test cell produced non-spherical and comet-like bubble clusters. The precise reasons behind the absence of recorded nuclear emissions is unknown at present but, as mentioned before, it appears to be closely tied with the behavior of the bubble clusters themselves. Spherical cluster implosions tend to result in nuclear emissions, whereas, non-spherical clusters (especially those tending to comet-like shapes) do not. Nevertheless, nuclear emissions were never noted for control experiments (i.e., with non-deuterated liquids) and also for experiments with water.

For unsuccessful campaigns on any given day the test cell operation would result in comet-like bubble streamer formations which would tend to persist despite operation for several hours. This required dismantling of the test reactor to seal leakage pathways, and to filter the test liquid for impurities, or, for persistent problems it was necessary to use a new batch of freshly-drawn test liquids. This is suspected to also be due to chemical byproducts of cavitation, and implies the need to study the chemistry of the process further to ensure improved repeatability. For successful campaigns, the test cell operation resulted initially in gassy comet-like structures during which null results were noted during trials. Upon continual degassing for (assuming other parameters such as liquid height and loss of vacuum do not impede) the comet-like structures would then reduce in quantity and individual spherical-looking bubble clusters are formed upon which the trial observations (over 25 to 50 seconds each) begin to indicate neutron emission when cavitation was on versus off. Thereafter, the CR-39 track samples were affixed and data acquisition was initiated and acquired electronically for the next several hours. Care was taken to ensure that the background conditions in the laboratory remained the same. During a typical campaign results were obtained in cycles; first with cavitation turned on for 100 to 300 seconds and then cavitation was turned off for 100 to 300 seconds. The cycles were repeated systematically. For successful campaigns, it was noted that the variation in the neutron emission (output for deuterated cases with cavitation on) for over 2h or so of operation fluctuated modestly (within +/- 20% of the mean), whereas, the background which was monitored continuously (i.e., in between every successive cavitation on runs) would remain well within 1 to 2 SD of the background counts.

Results with BF_3 Thermal Neutron Detector

A BF_3 nuclear particle detector (length=4.5cm; diameter = 1.25 cm) was used with a 20 cm diameter paraffin ball moderator over it to enhance thermal neutron fluxes since BF_3 has a high cross-section for absorption only for low-energy neutrons. The BF_3 detector was calibrated for efficiency of detection and also with distance using a NIST certified Pu-Be source (emitting ~ 2 x 10^6 n/s) as well as with 1 μCi Co-60 and Cs-137 gamma ray sources. Results are shown in Fig. 2a. Results of pulse-height spectra obtained with the Pu-Be source show a well defined neutron peak above channel 25. At a 10 cm separation

the count rate was ~ 220 c/s which, when corrected for solid angle (0.0054), gives an intrinsic efficiency of ~3% for the detection of fast neutrons in the MeV range. The nonlinear variation of neutron counts with distance reasonably corresponds to the inverse square law (with deviations that may primarily be attributed to multi-dimensional aspects). Figures 2b and 2c show pulse-height spectra with and without the paraffin moderator for cases where only the Co-60 and Cs-137 sources were present. As noted, the higher energy (~1.3 MeV) gamma rays from Co-60 lead to larger pulse heights than the 0.66 MeV gamma rays from Cs-137. Nevertheless, the majority of pulses due to gamma ray interactions occur below channel 20. This gave us confidence that this detector system could be used reliably to simultaneously measure neutrons with good separation from gamma rays.

Results from nuclear particle-nucleated cavitation tests shown in Figures 3 to 4 and in Table 1 were obtained with a BF_3 thermal neutron detector (TND) at an approximate distance of 30cm from the test cell. Data were taken over an aggregate time of 7,200 s (i.e., 3,600 s with cavitation and 3,600 s with cavitation off) for each test liquid mixture. Data presented represent a total of twenty-four (24) runs in 12 cycles (each cycle conducted over a span of 300 s first with cavitation on and then for 300 s with cavitation turned off). It is clearly seen that experiments with the control fluid mixture C_6H_6-C_2Cl4-C_3H_6O-UN did not result in any statistically significant change in counts over background. In contrast, the results of experiments with the deuterated mixture C_6D_6-C_2Cl_4-C_3D_6O-UN produced a statistically significant [~ 6 standard deviation (SD)] emission, with ~ 400% increases in neutron counts and ~100% increases of gamma ray counts. As a cross-check, the distance of the detector from the test cell was roughly doubled from a nominal ~30-35cm to about 65-70 cm and the experiments were repeated. Results are shown in Figure 5 where we see that the increase of neutron counts has come down considerably displaying the expected non-linear dependence with distance.

The experiments described above were also conducted by dissolving UN in heavy and ordinary water *(14)*. Results are shown in Figures 6 through 7. For these experimental parameters there was no statistically significant evidence of nuclear emissions with cavitation, for either H_2O or D_2O, which was in accordance with our expectations *(1(b), 3*).

Results with Liquid Scintillation (LS) Detector

In order to ascertain the energy of the emitted neutrons, the data obtained with the BF_3 detector system were complemented with data taken with a 5cm diameter x 5cm long LS detector *(2)* with pulse-shape discrimination (PSD) between neutrons and gamma rays as seen from Figure 8a (where with PSD gamma rays are virtually eliminated). Using well-established light curves *(7-9)* and with the instrument settings used for the reported experiment data, the 2.45 MeV proton recoil edge (PRE) corresponded to channels between ~110-120 based on Co-60 and Cs-137 gamma ray source pulse-height data shown in Figures 8b and 8c.

The data in Figures 9 and 10 and in Table 1 are typical of the trends observed when the test cell was operating largely without formation of non-spherical streamers or comet-like structures. That is, while statistically significant increases of ~20 SD could be obtained (Figure 9b) within a single run of 300 s for the deuterated liquid (i.e., taken over a time span of 300 s with cavitation turned on and then for 300 s with cavitation turned off), the corresponding changes for non-deuterated liquid were within 1 SD (Figure 9a). The background varied in the course of data acquisition campaigns by about 1 to 2 SD. It is emphasized that several sets of data were obtained alternately over time spans of 100 s and 300 s each with cavitation turned on and cavitation turned off, respectively. Futhermore, for the specific instrument settings and calibrations done during such a campaign a series of runs were conducted for the deuterated and non-deuterated liquid mixtures. Aggregate results obtained over 3,000 s with the C_6D_6-C_2Cl_4-C_3D_6O-UN mixture, and separately over 2,200 s with the control mixture C_6H_6-C_2Cl_4-C_3H_6O-UN are shown in Figures 10 through 12. The results shown in Figure 10 are composed of 10 runs (i.e., two sets of runs each taken alternately over a span of 100 s with cavitation on and then for 100 s with cavitation off, plus three sets of runs each taken alternately over a span of 300 s with cavitation on and then for 300 s with cavitation off). The results shown in Figure 11 are composed of 14 runs (i.e., three sets of runs each taken alternately over a span of 100 s with cavitation on and then for 100 s with cavitation off, plus four sets of runs each taken alternately over a span of 300 s with cavitation on and then for 300 s with cavitation off). The aggregate data are even more compelling. We notice ~ 30 SD increase of neutron emission for experiments with C_6D_6-C_2Cl_4-C_3D_6O-UN mixture, but virtually no significant change for the control liquid. The maximum neutron energy is seen from Fig. 12 to correspond to $\leq$ 2.45 MeV, indicative of D-D nuclear fusion.

Notes on Neutron Track Detector Usage

Neutron track (NT) detectors have been used for over 40 years *(10,11)* as a passive means for directly confirming and leaving unambiguous "physical" evidence for the presence of neutrons. In these detectors, the interaction of a neutron with elements such as H, C, O, etc. in the detector material leaves a permanent mark in the form of a track that become visible when the material is etched. One well-established and widely used material is allyl diglycol carbonate (CR-39) plastic. CR-39 NT particle detectors (each of length = 2cm; width = 1cm; thickness = 1mm; net track viewing area ~ $1cm^2$) were procured (*12*) for use in our experiments to derive direct, unambiguous physical evidence of fast neutrons. It is well-known that CR-39 detectors are completely insensitive to gamma rays and are largely sensitive only to MeV level (fast) neutrons.

The procured CR-39 detector chips were carefully calibrated using a 1 Ci NIST certified Pu-Be neutron source (emitting ~ $2x10^6$ n/s). The CR-39 detector was attached directly to the side of the Pu-Be source (diameter = 18.8 mm; height=53 mm) and radiated for 100 seconds prior to etching for prescribed times in a solution of water and KOH at ~80^oC. While affixing to either the Pu-Be source or to the test cell, the plastic covering in which they were delivered by the manufacturer was kept in place. Scotch tape was first placed on to the cleaned test cell surface upon which the CR-39 chip with it's plastic

covering intact was placed, after which the assembly was taped over by another piece of scotch tape. After irradiation the chip was detached. Thereafter, the plastic cover sheets were removed from either side. The chips were then placed in the water bath for etching. Table 2 shows the variation of neutron tracks with etch time and several other parameters. It is to be noted that pre-existing (background) nuclear track counts from batch to batch from the supplier can vary. Whereas, for the first batch the average was around 13 (+/- 2), the second batch showed an average background of ~19 (+/- 2) tracks. While there can be some subjectivity involved (due to presence of scratches or other stains during fabrication), neutron tracks were consistently determined as being those that were clearly spherical or elliptical (to account for angular strike from neutrons) with sharply-defined boundaries and grayish to dark interior. Viewing for tracks was conducted using an optical microscope from the side facing the test cell (i.e., the side which was affixed to the test cell). The track counts obtained compared well against published results (*10,11*) confirming a fast neutron detection efficiency of ~ 3-5x10^{-5}. As noted therein, the detection efficiency increases with etch time. Thereafter, the CR-39 NT detectors were utilized in a series of self nucleated acoustic cavitation experiments with deuterated and control (non-deuterated) liquids.

Data from a range of various tests are tabulated in Table 2 and overall results are shown in Figure 13. It was verified that no statistically significant change occurs over background levels without cavitation in deuterated liquid. Significantly, close to a 100% increase (and > 5 SD) in visible neutron tracks were observed for individual samples, only for samples associated with self-nucleation based cavitation experiments in the deuterated liquid C_6D_6-C_2Cl_4-C_3D_6O-UN experiments. On the aggregate, the production of neutron tracks for the deuterated liquid amounted to a ~14 SD change, whereas, for the control liquid C_6H_6-C_2Cl_4-C_3H_6O-UN the changes were within 0.5 SD.

Notes on Gamma Ray Spectra Data

Gamma ray spectra were also obtained to understand better the neutron emission data from the alpha particle recoil induced nucleation experiments. A Harshaw^{TM} NaI (5cm diameter x 13cm length) detector mounted on a Canberra 2007P base was utilized for this purpose. The detector was calibrated using a 1 μCi Co-60 source for which the pulse height spectrum was obtained and shown in Fig. 14. As noted, although the energy resolution is not as good as one may expect for a Ge-type detector an accumulation of counts is noted between channels 5 to 15. Thereafter, data were taken with and without cavitation for experiments with benzene-C_2Cl_4-Acetone-UN mixtures. Results are presented in Figures 15 through 16. The results of the control experiments with and without cavitation using C_6H_6-C_2Cl_4-C_3H_6O-UN indicated no statistically significant change between cavitation on and off. In contrast, the results for the experiments with and without cavitation using C_6D_6-C_2Cl_4-C_3D_6O-UN showed a noticeable (~ 2 SD) increase in gamma ray emissions above background with cavitation on versus off. This was especially noteworthy as seen from Figure 15 for the region which correlates with emissions of ~1 MeV photons. The ~1 MeV region's accumulation of counts may be attributed to gamma emissions when neutrons get absorbed in the chlorine atoms of the

test liquid (which has a large cross-section of about 33 barns). Such emissions were not observed for experiments with non-deuterated liquid mixtures. These data confirm that neutron emissions during self nucleation experiments will also be accompanied with limited gamma ray emissions due to neutron interactions with atoms of the test fluid.

Notes on nuclear emissions due to dissolved uranyl nitrate

An assessment was conducted to gage the potential for neutron emissions from the uranium decay related alpha particle interactions with ^{13}C (about 1% of C atoms are well-known to be of the ^{13}C isotope). Such interactions have a fairly low efficiency of neutron production quoted as ~ 1 neutron for every 10^5 alpha particles *(8)*. Taken together with the ~$4.5x10^9$y half-life of ^{238}U the presence of up to 7g of uranyl nitrate in solution can at most result in a small alpha-interaction based neutron production rate of ~0.005 n/s. Since this is spread over a test cell surface area of about 100 cm^2 the resulting flux would amount to ~ $5x10^{-5}$ n/cm^2-s. This is well below the background cosmic flux *(8)* at sea level of about 1 n/cm^2-s. Another possible mechanism could result from the spontaneous fission of ^{238}U with a half-life of $6.5x10^{15}$y. This too results in a flux of ~ 3 x 10^{-4} n/cm^2-s. Therefore, we can safely conclude that the presence of dissolved uranium nitrate salt can not result in any discernible neutron emissions and are several orders of magnitude lower than the observed neutron emission rate of $5x10^3$ to 10^4 n/s.

Acknowledgment:

The work reported in this manuscript was supported by the State of Indiana (Purdue University). The initial suggestions for utilizing deuterated benzene and for striving to conduct experiments without use of external neutrons were made by Prof. W. Bugg and are most appreciated. The in-depth advice and ongoing technical assistance and cross-checks provided for successful conduct of this study by Dr. JaeSeon Cho of Oak Ridge National Laboratory are gratefully acknowledged and appreciated. The timely support provided by Purdue University's Radiological and Environmental Management services group for conduct of experiments, Dr. Roger Stevens of Spectrum Techniques, Dr. Charles Hurlbut of Eljen,Inc., Ed Bickel of Channel Industries, and Luke Carr of Landauer, Inc., discussions on track detectors with Prof. R. Fleisher as well as the insightful review and comments from Michael Murray of BWXT-Y12 are acknowledged.

References

1a. R. P. Taleyarkhan, C. D. West, J. S. Cho, R. T. Lahey,Jr., R. I. Nigmatulin and R. C. Block, *Science*, Vol.295, 1868-1873, (March 8, 2002).

1b R. Nigmatulin, R. T. Lahey, Jr. and R. P. Taleyarkhan, "The Analysis of Bubble Implosion Dynamics," *Science Online*, www.sciencemag.org /cgi/content /full /295 /5561 /1868/DC1, (March 8, 2002).

2. R. P. Taleyarkhan, J. S. Cho, C. D. West, R. T. Lahey,Jr., R. I. Nigmatulin and R. C. Block, *Phys. Rev. E*, Vol.69, 036109, (March, 2004).

3. Nigmatulin, R.I., et al., *Physics of Fluids*, **17**, 107106 (2005).

4. Nigmatulin, R.I., R. T. Lahey, Jr., and R. P. Taleyarkhan, *Journal of Power and Energy*, Vol.218, part A, 345-364, (2004).

5. Y. Xu, and A. Butt, *Nuclear Engineering and Design*, Vol. 235-3, 1317-1324 (2005).

6. Lahey, R.T., Jr., R.I. Nigmatulin, R.P. Taleyarkhan and I. Akhatov, "Sonoluminescence and the Search for Sonofusion," *Advances in Heat Transfer*, Academic Press, Vol. 35 (2005).

7. N. P. Hawkes et al., *Nuclear Instrumentation & Methods in Physics Research*, Vol. 476, 190-194 (2002).

8. G. F. Knoll, *Radiation Detection and Measurement,* Wiley, New York, (1989).

9. J. Harvey and N. Hill, *Nucl. Instrum. Methods Phys. Res.*, Vol. 162, 507 (1979).

10. Fleischer, R. L., P. B. Price, and R. M. Walker, "Nuclear Tracks in Solids," University of California Press, Berkeley, 1965

11. Fleischer, R. L., L. G. Turner, H. G. Paretzke and H. Schraube, "Personnel Neutron Dosimetry Using Particle Tracks in Solids: A Comparison," *Health Physics*, Vol. 47, No. 4 (1984).

12. The CR-39 NT detectors were purchased from Landauer, Inc. Etching was performed using a H_2O-KOH solution (1 part in 3 of KOH by mass) at 80 C.

13. A 580 cc batch was first prepared combining 250 cc of benzene, 250cc of tetrachloroethylene and 80cc of acetone to which ~7g of uranyl nitrate was added. About 400cc were typically utilized during each experiment.

14. About 3g of natural uranyl nitrate was added to 300cc of water for self-nucleation tests.

Table 1. Count Statistics (above background)							
Figure No.	Cav. On Counts	Cav. Off Counts	Difference (On-Off)	S.D. in Difference	Diff/SD	Detector	Fluid
3	50	49	-1	10	-0.10	BF_3	$C_6H_6+C_2Cl_4+C_3H_6O$+UN
4	124	49	75	13.2	5.7	BF_3	$C_6D_6+C_2Cl_4+C_3D_6O$+UN
5	52	44	8	9	0.9	BF_3	$C_6D_6+C_2Cl_4+C_3D_6O$+UN (Distance = 65-70 cm)
~~6~~	39	44	-5	9.1	-0.55	BF_3	H_2O+UN
~~7~~	37	39	-2	8.8	-0.23	BF_3	D_2O+UN
~~9~~a	913	923	-10	43	-0.23	LS	$C_6H_6+C_2Cl_4+C_3H_6O$+UN
9b	2051	1055	966	55	17.4	LS	$C_6D_6+C_2Cl_4+C_3D_6O$+UN
10	3488	3265	123	82	1.5	LS	$C_6H_6+C_2Cl_4+C_3H_6O$+UN
11	10157	5007	5150	173	29.8	LS	$C_6D_6+C_2Cl_4+C_3D_6O$+UN
13	Table 2	Table 2	Table 2	Table 2	~0.5	Track	$C_6H_6+C_2Cl_4+C_3H_6O$+UN
13	Table 2	Table 2	Table 2	Table 2	14	Track	$C_6D_6+C_2Cl_4+C_3D_6O$+UN
15a	16804	16906	-102	182	-0.57	NaI	$C_6H_6+C_2Cl_4+C_3H_6O$+UN
15b	16196	15844	352	178	2	NaI	$C_6D_6+C_2Cl_4+C_3D_6O$+UN

Table 2. Summary of Neutron Track Data

CR-39 batch / Etch Time(h)	Detector Position	Liquid	Cavitation	Tracks*	Change over background	Notes
1 / (3h)	On test cell	C_6D_6+C_2Cl_4+C_3D_6O+UN	No	14	~ 0	No change without cavitation
1 / (3h)	a)Background b)On test cell c)On test cell	C_6H_6+C_2Cl_4+C_3H_6O+UN	a)N/A b)Yes (2h) c)Yes (2h)	a)15 b)14 c)16	 -1 1	Change within 1 SD
1 / (3h)	a)Background b)On test cell c)On test cell	C_6H_6+C_2Cl_4+C_3H_6O+UN	a)N/A b)Yes (2h) c)Yes (2h)	a)12 b)11 c)14	 -1 2	Change within 1 SD
1 / (3h)	a)Background b)On test cell c)On test cell	C_6D_6+C_2Cl_4+C_3D_6O+UN	a)N/A b)Yes (2h) c)Yes (2h)	a)13 b)22 c)25	 9 12	~ 100% increase over background
1 / (3h)	a)Background b)On test cell c)On test cell	C_6D_6+C_2Cl_4+C_3D_6O+UN	a)N/A b)Yes (2h) c)Yes (2h)	a)11 b)23 c)27	 12 16	~ 100% average increase over background
1 / (14h)	a)Background b)On test cell	C_6H_6+C_2Cl_4+C_3H_6O+UN	a)N/A b)Yes (2h)	a)104 b) 97	 -7	Change within 1 SD
1 / (8h)	a)Background b)On test cell c)On test cell	C_6D_6+C_2Cl_4+C_3D_6O+UN	a)N/A b)Yes (2h) c)Yes (2h)	a)61 b)89 c)98	 28 37	~ 60% average increase over background; ~ 5 SD increase.
1 / (14h)	a)Background b)On test cell	C_6D_6+C_2Cl_4+C_3D_6O+UN	a)N/A b)Yes (2h)	a)115 b) 154	 49	~50% increase over background; ~ 5 SD increase.
2 / (3h)	a)Background b)On test cell c)On test cell	D_2O+UN	a)N/A b)Yes (2h) c)Yes (2h)	a)20 b)19 c)21	 -1 +1	Changes within 1 SD
2 / (3h)	a)Background b)On test cell c)On test cell	C_6D_6+C_2Cl_4+C_3D_6O+UN	a)N/A b)No c)No	a)19 b)21 c)18	 2 -1	Change within 1 SD
2 / (3h)	a)Background b)On test cell c)On test cell	C_6D_6+C_2Cl_4+C_3D_6O+UN	a)N/A b)Yes (2h) c)Yes (2h)	a)17 b32 c)27	 15 10	~ 90% average increase over background.
2 / (3h)	a)Background b)On test cell	C_6D_6+C_2Cl_4+C_3D_6O+UN	a)N/A b)Yes (2h)	a)19 b)27	 8	~ 50% increase over background.
1 / (3h) (6h) (14h)	Detector on 1 Ci Pu-Be source (OD= 1";H=1.5") for 100s	N/A	N/A	397 (3h) 579 (6h) 1544(14h)	N/A	Track counts intrinsic efficiency is similar (~ $5x10^{-5}$) to reported values (Fleischer et al; Ref. 11)
(*) – Note correspondence of background tracks with the supplier's batch number mentioned in column 1						

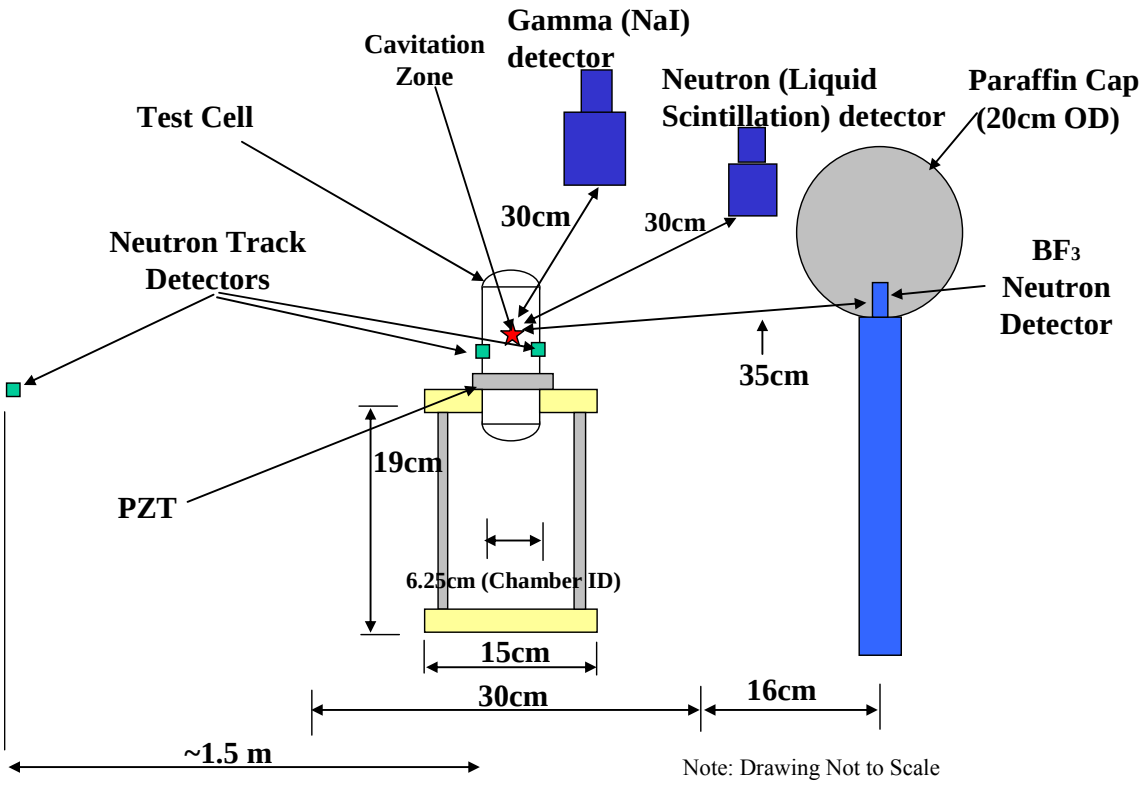

Figure 1. Schematic representation of experimental setup.

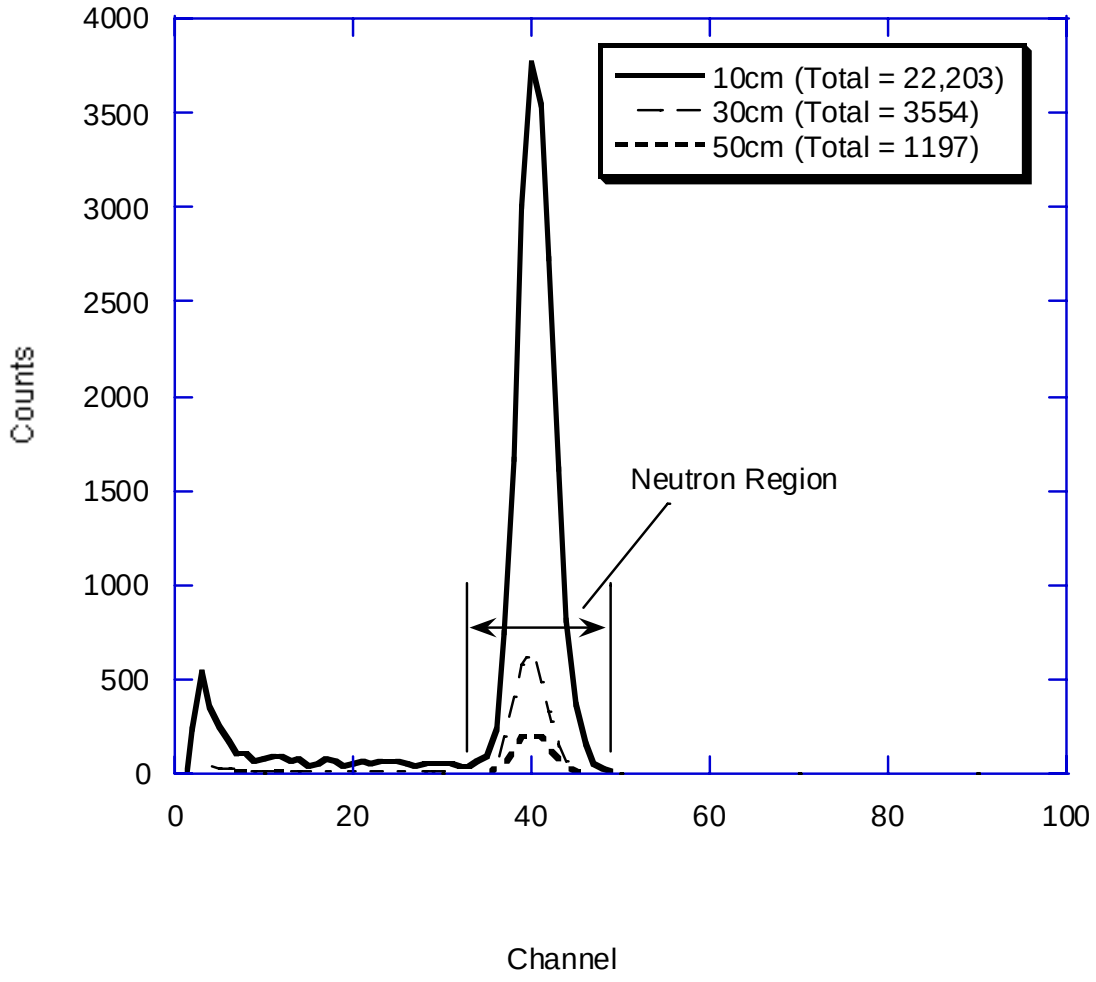

Figure 2a. Calibration neutron spectrum with 1 Ci ($2x10^6$ n/s) Pu-Be source and BF_3 detector (All data taken over 100 seconds).

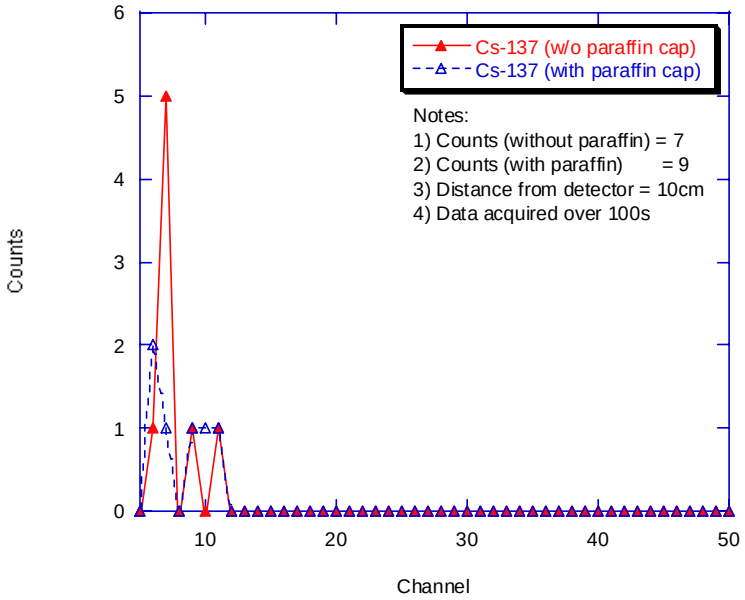

(b)

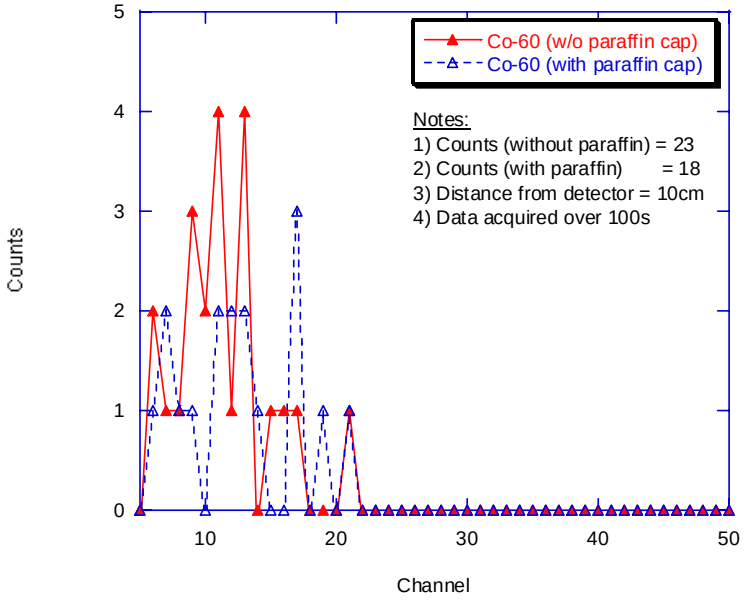

(c)

Figure 2b,c Calibration spectra for Co-60 and Cs-137 using BF_3 detector (with and without paraffin cap)

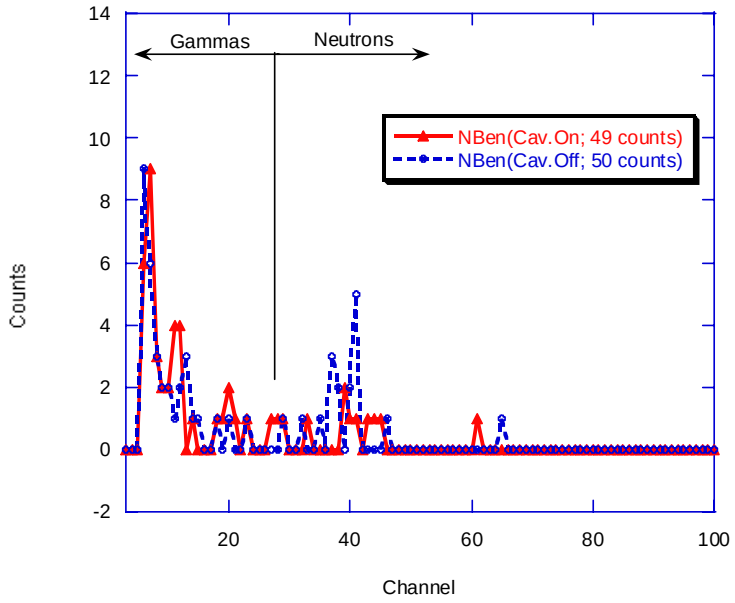

(a)

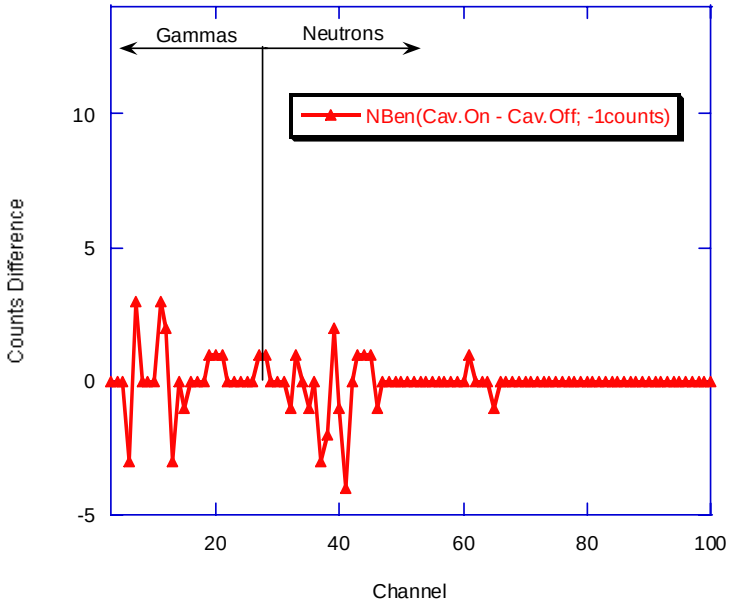

(b)

Figure 3a,b Neutron-Gamma Spectra for C_6H_6-C_2Cl_4-C_3H_6O-UN with self nucleation and BF_3 detector. Data represent a total of twenty-four (24) runs in 12 cycles (each cycle conducted over a span of 300 s first with cavitation on and then for 300 s with cavitation turned off). Total time = 7,200 s.

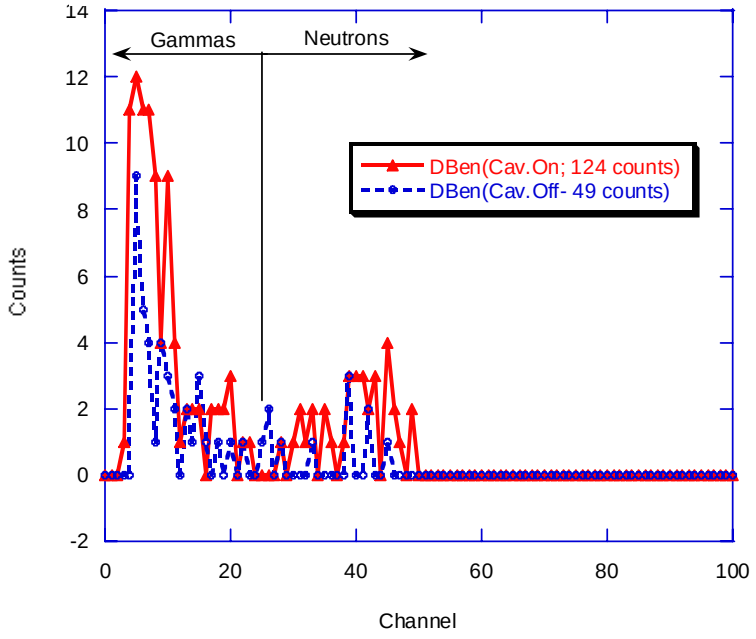

(a)

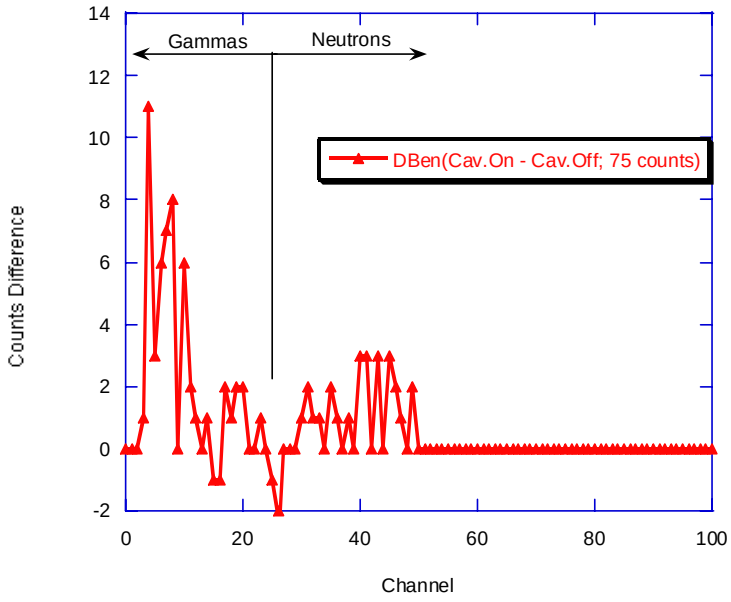

(b)

Figure 4a,b Neutron-Gamma Spectra for C_6D_6-C_2Cl_4-C_3D_6O-UN with self nucleation and BF_3 detector. Data represent a total of twenty-four (24) runs in 12 cycles (each cycle conducted over a span of 300 s first with cavitation on and then for 300 s with cavitation turned off). Total time =7,200 s.

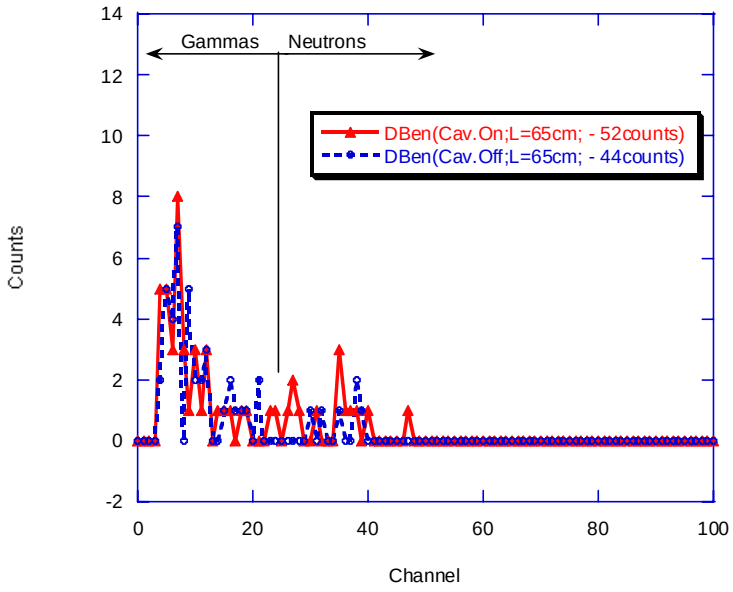

(a)

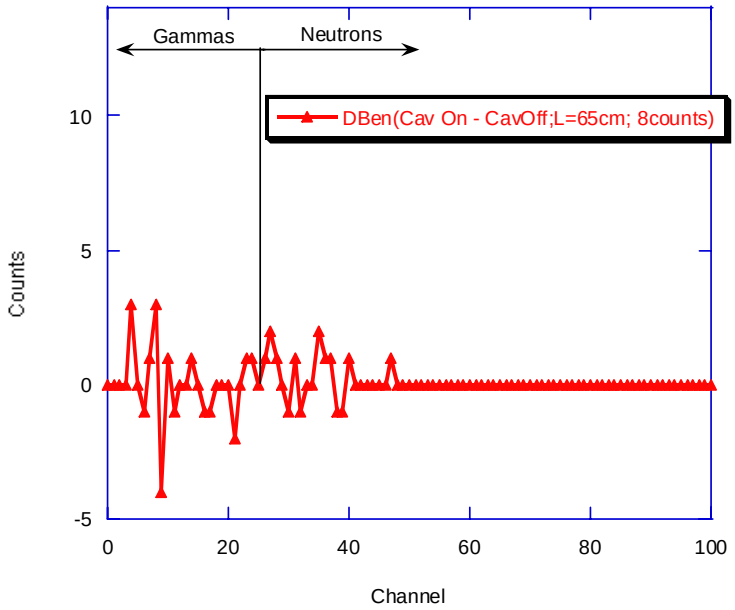

(b)

Figure 5a,b Neutron-Gamma Spectra for C_6D_6-C_2Cl_4-C_3D_6O-UN with self nucleation and BF_3 detector. Distance from test cell = ~65 cm. Data represent a total of twenty (20) runs in 10 cycles (each cycle conducted over a span of 300 s first with cavitation on and then for 300 s with cavitation turned off). Total time = 6,000 s.

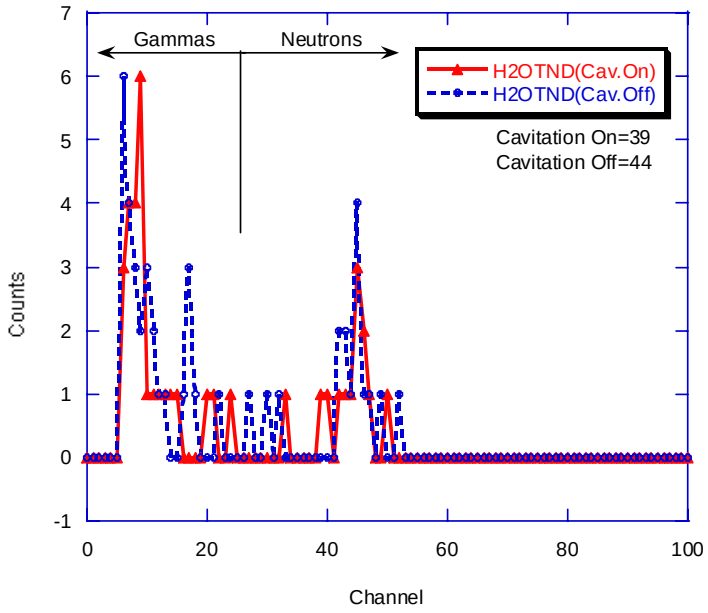

(a)

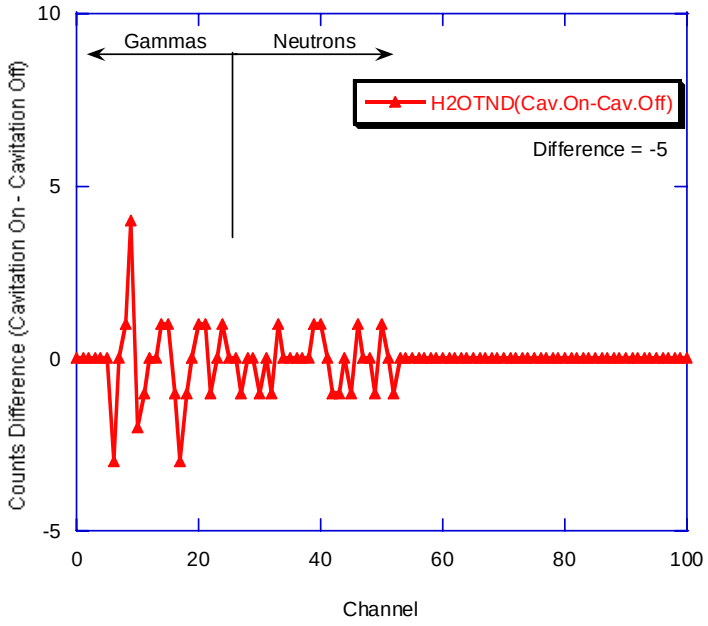

(b)

Figure 6a,b Neutron-Gamma Spectra for H_2O with self nucleation and BF_3 detector. Data represent a total of ten (10) runs in 5 cycles (each cycle conducted over a span of 300 s first with cavitation on and then for 300 s with cavitation turned off). Total time = 3,000 s.

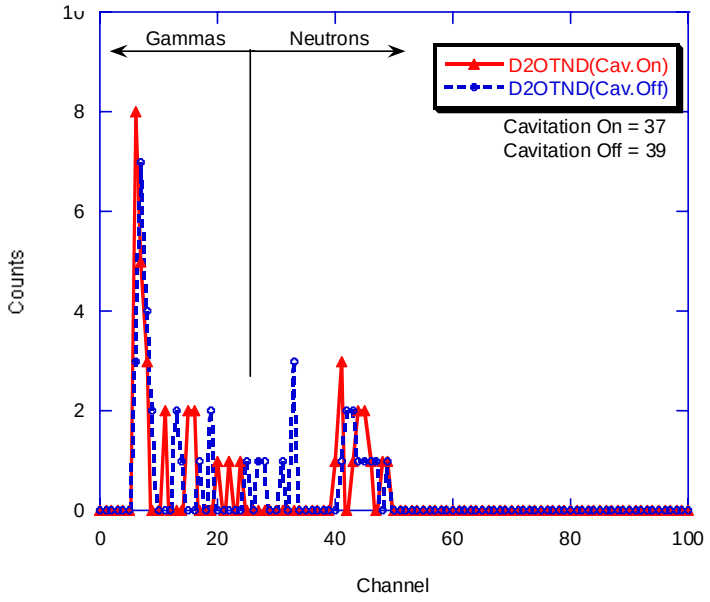

(a)

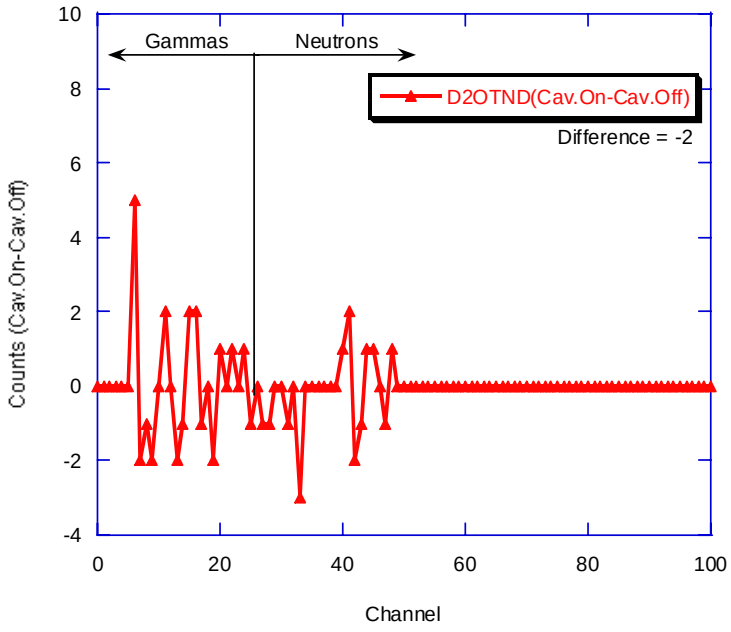

(b)

Figure 7a,b Neutron-Gamma Spectra for D_2O with self nucleation and BF_3 detector. Data represent a total of ten (10) runs in 5 cycles (each cycle conducted over a span of 300 s first with cavitation on and then for 300 s with cavitation turned off). Total time = 3,000 s.

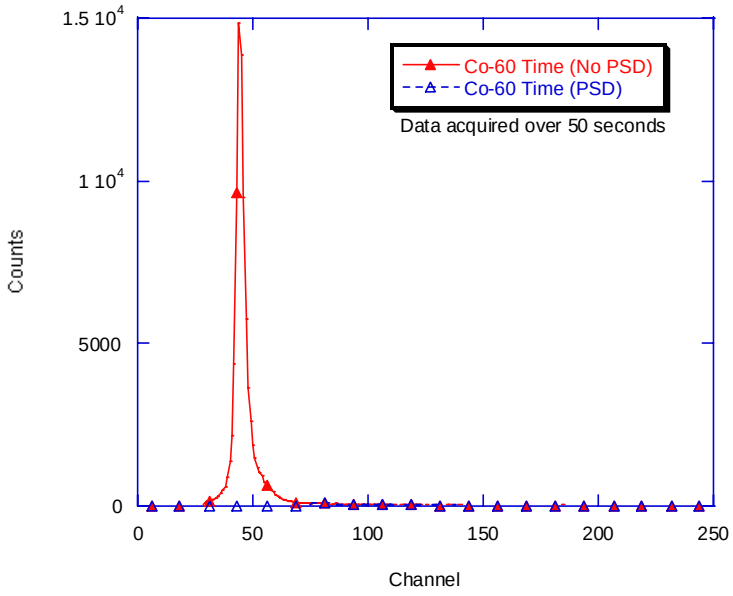

(a)

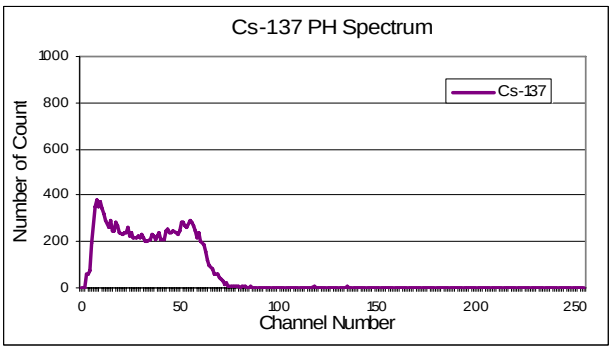

(b)

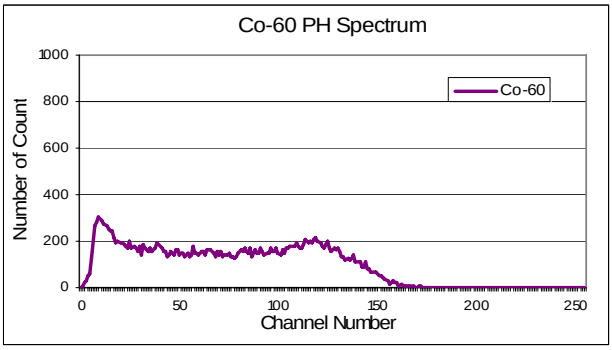

(c)

Figure 8 Pulse-shape discrimination (a), and pulse height spectra (b,c) taken with LS Detector

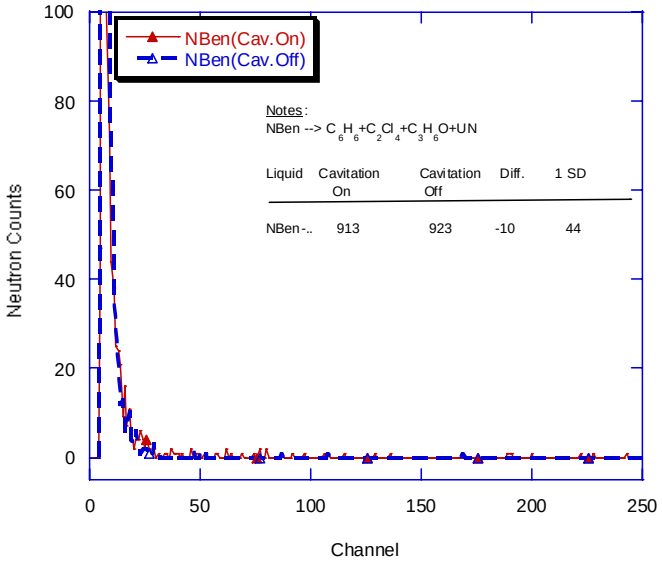

Figure 9a. Representative pulse height spectra for C_6H_6-C_2Cl_4-C_3H_6O-UN mixture with self nucleation and LS detector. Data collected over 300 seconds with cavitation on followed by data taken over 300 s with cavitation off.

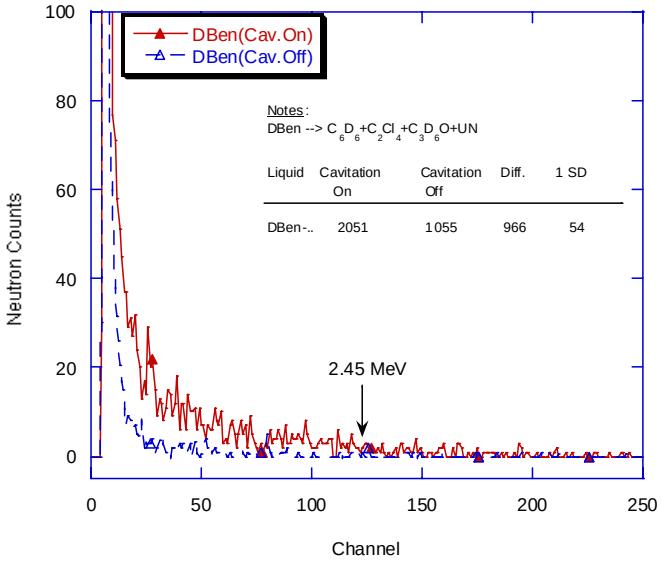

Figure 9b. Representative pulse height spectra for C_6D_6-C_2Cl_4-C_3D_6O-UN mixture with self nucleation and LS detector. Data collected over 300 seconds with cavitation on followed by data taken over 300 s with cavitation off

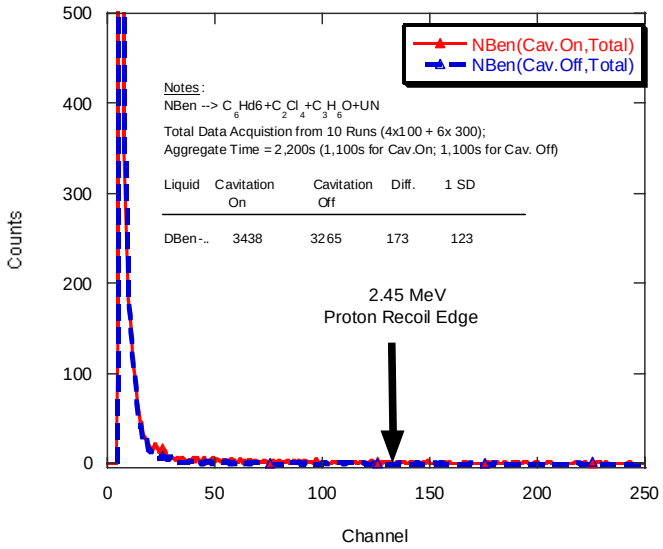

Figure 10 Aggregate pulse height spectra for C_6H_6-C_2Cl_4-C_3H_6O-UN mixture with self nucleation and LS detector. Data represent a total of ten (10) runs in 5 cycles (each cycle conducted over a span of 100 s or 300 s first with cavitation on and then for 100 s or 300 s with cavitation turned off). Total time =2,200 s.

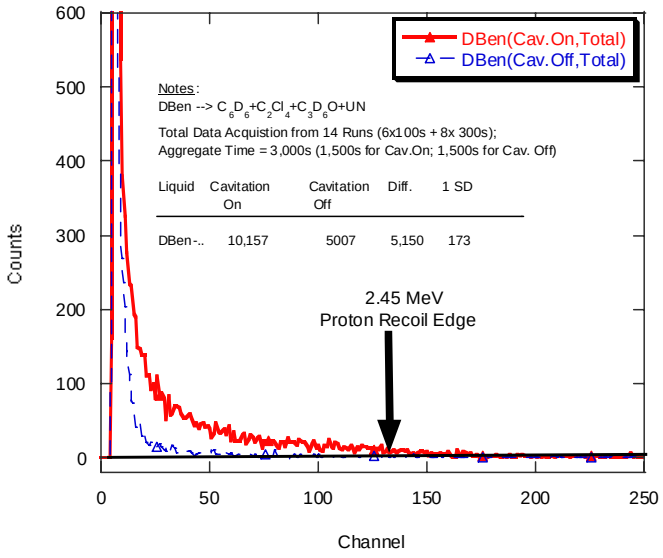

Figure 11 Aggregate pulse height spectra for C_6D_6-C_2Cl_4-C_3D_6O-UN mixture with self nucleation and LS detector. Data represent a total of fourteen (14) runs in 7 cycles (each cycle conducted over a span of 100 s or 300 s first with cavitation on and then for 100 s or 300 s with cavitation turned off). Total time =3,000 s.

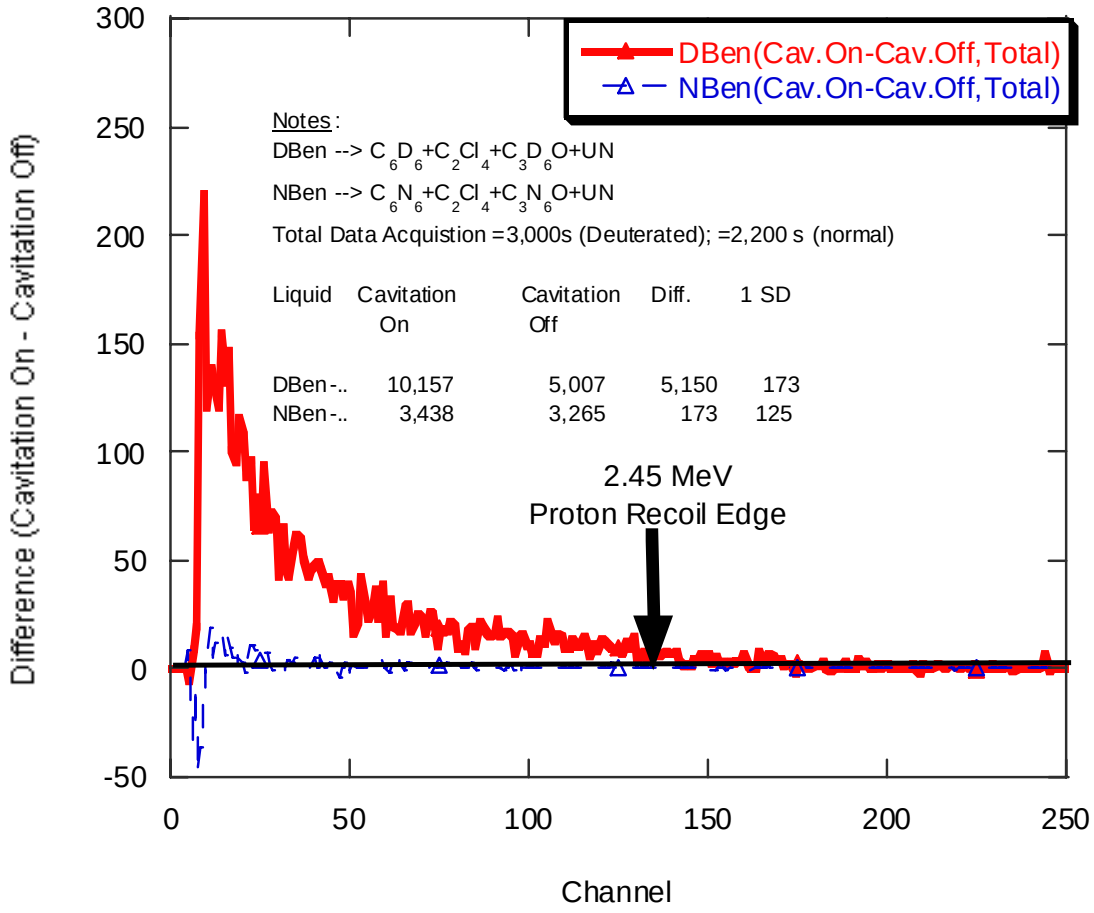

Figure 12 Aggregate change in counts from pulse height spectra (in Figures 10 and 11) for C_6D_6-C_2Cl_4-C_3D_6O-UN and C_6H_6-C_2Cl_4-C_3H_6O-UN mixtures with self nucleation and LS detector

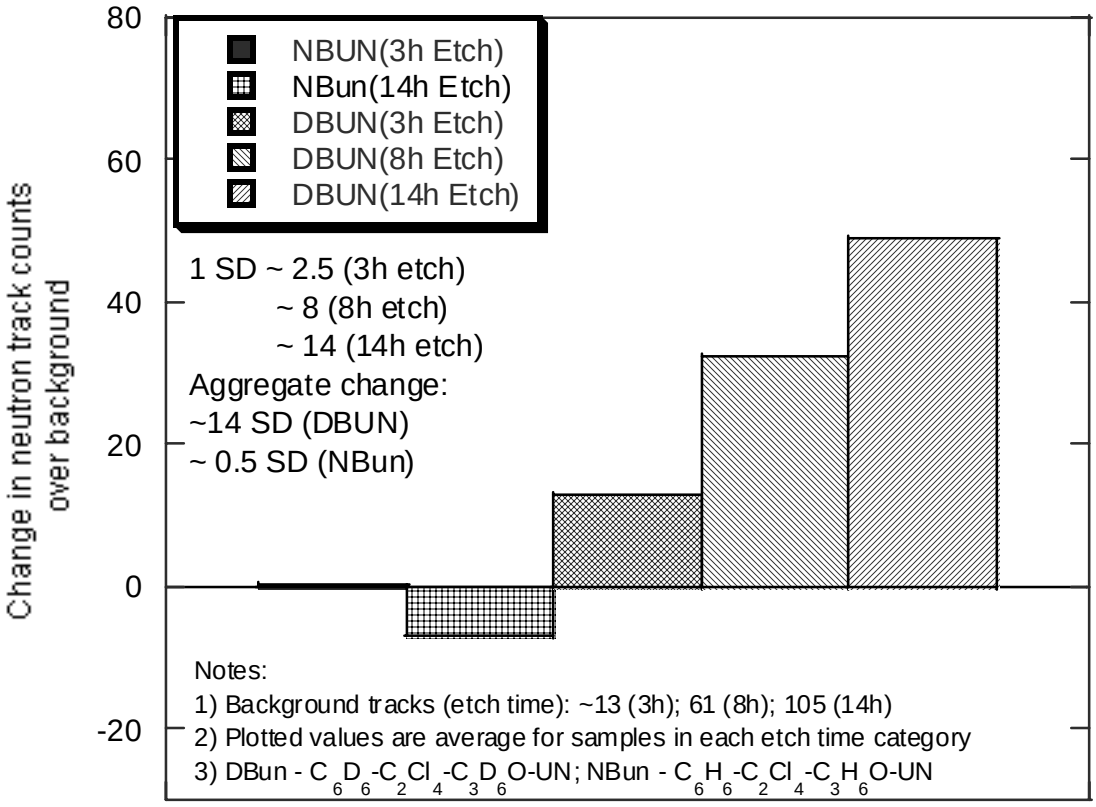

Figure 13. Variation of neutron tracks for deuterated and non-deuterated test liquids.

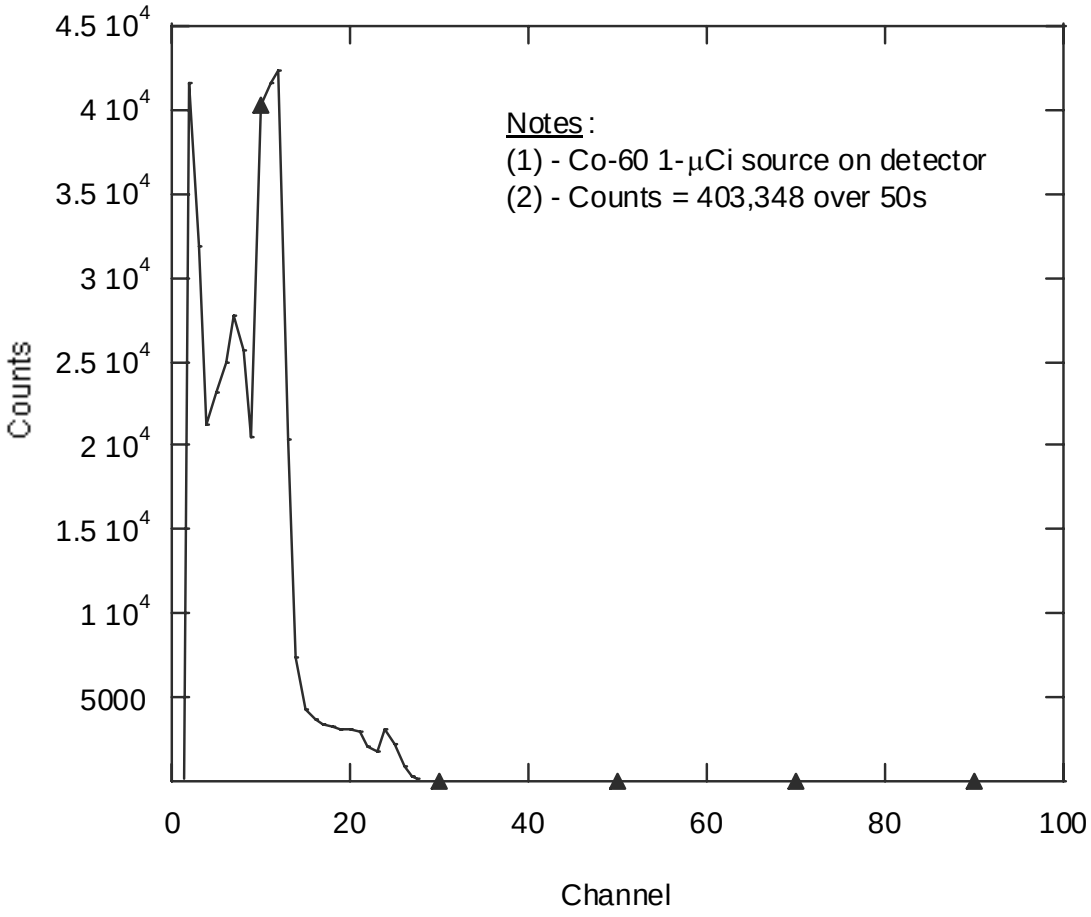

Figure 14. Calibration spectra with NaI detector using Co-60 (data taken over 50s).

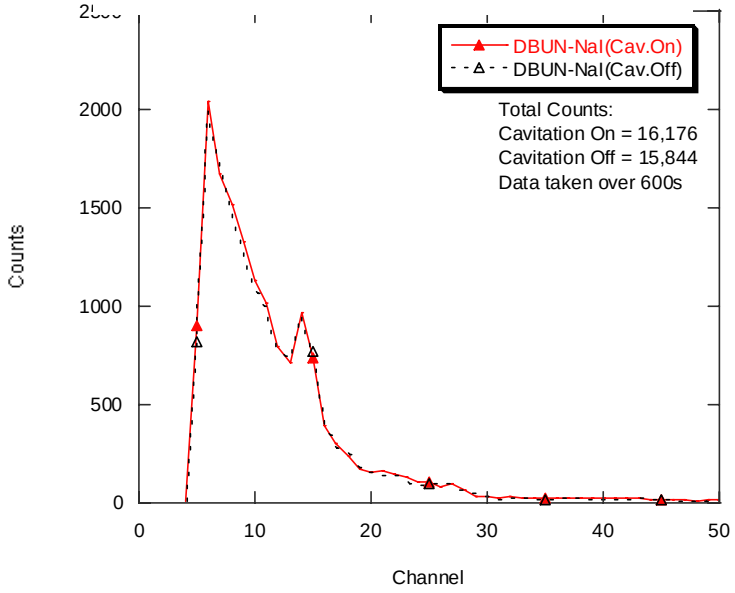

(a)

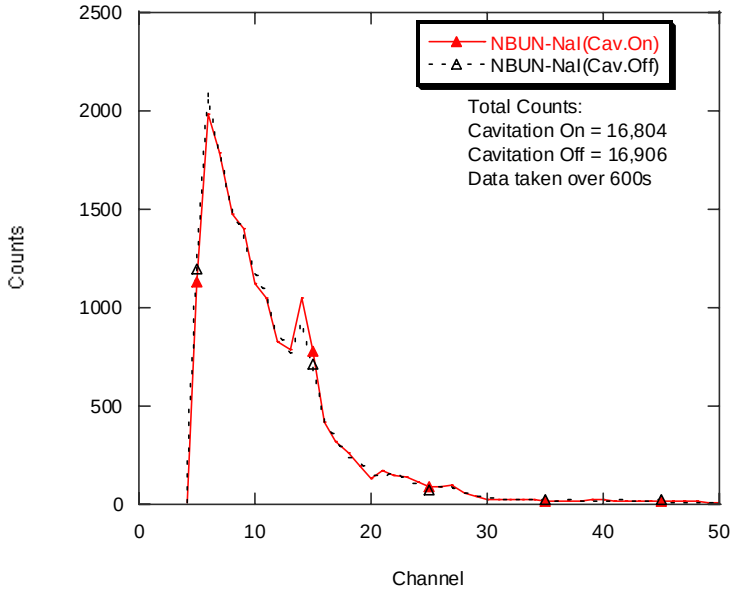

(b)

Figure 15a,b. NaI detector gamma spectra for C_6D_6-C_2Cl_4-C_3D_6O-UN (DBUN) and C_6H_6-C_2Cl_4-C_3H_6O-UN (NBUN) mixtures with self-nucleated cavitation (data taken over 600s).

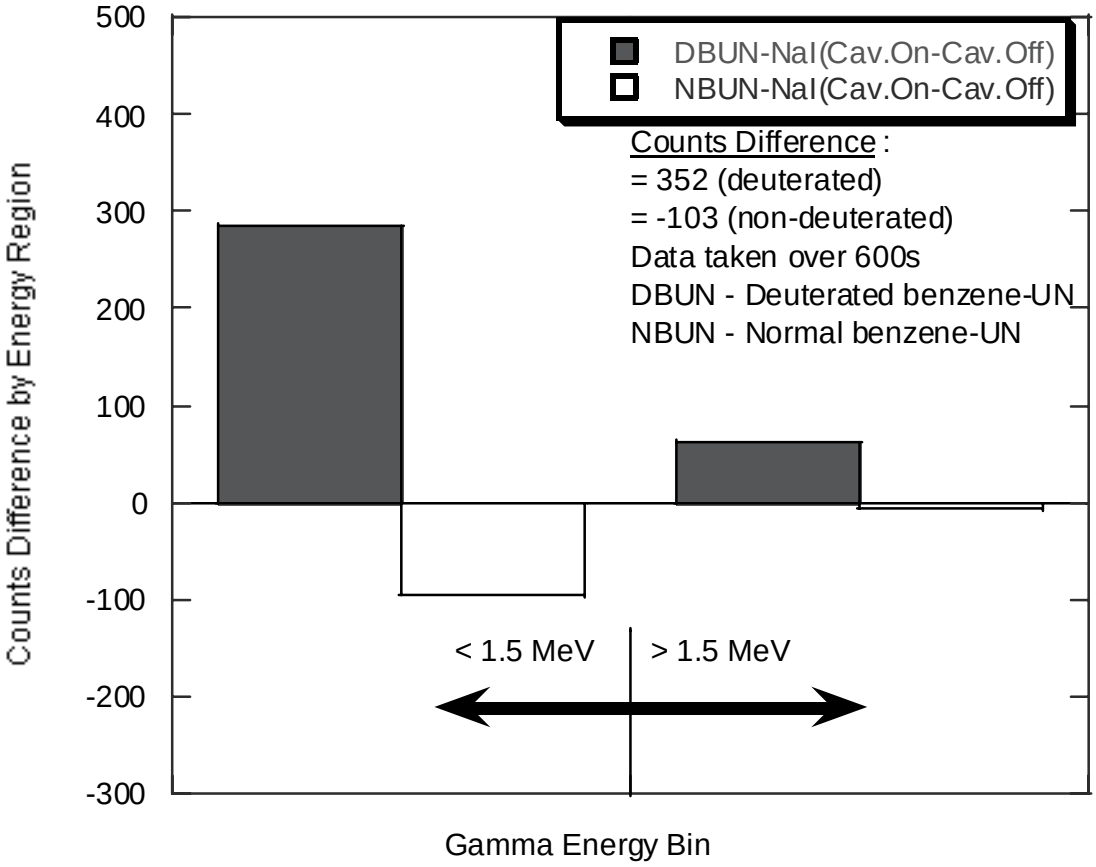

Figure 16. Variation of gamma energy spectra counts with NaI detector gamma spectra for C_6D_6-C_2Cl_4-C_3D_6O-UN mixture with self-nucleated cavitation (data taken over 600s).